Controlling the Specific CO 2 Adsorption on Electrochemically Formed Metallic Copper Surfaces

Alexis Grimaud, Wei Yin, Florent Lepoivre, Jean-marie Tarascon

Controlling the specific CO_2 adsorption on electrochemically formed metallic copper surfaces

Alexis GRIMAUD,[1,2*] Wei Yin,[1,3] Florent LEPOIVRE,[1,3] and Jean-Marie TARASCON[1,2,3,4]

1. Chimie du Solide et de l'Energie, UMR 8260, Collège de France, 75231 Paris Cedex 05, France
2. Réseau sur le Stockage Electrochimique de l'Energie (RS2E), FR CNRS 3459, 80039 Amiens Cedex, France
3. Sorbonne Universités – UPMC Univ Paris 06, 75005 Paris, France
4. ALISTORE-European Research Institute, FR CNRS 3104, 80039 Amiens, France

Corresponding author: alexis.grimaud@college-de-france.fr

Abstract

The recent demonstration of the reduced overpotential for the electrochemical conversion of CO_2 to CO on the surface of oxidized copper films raised the question of possible interplay existing between the electroreduction of copper to its metallic form and the adsorption of CO_2 on its surface. To study this effect and better understand the factor governing the CO_2 adsorption on the surface of copper-based catalysts, we studied different copper vanadates oxides known for their ability to form metallic copper particles on their surface by electroreduction in Li^+-containing salt. By controlling the vanadates framework, the potential at which metallic copper is formed can be controlled and selectively be varied around the CO_2/CO standard potential. Studying the reduction behavior of these phases in CO_2-saturated organic media containing Li^+-salt, we demonstrate that the CO_2 adsorption is correlated with the potential at which Cu particles are electrochemically formed. We further show that the CO_2 adsorption is correlated with the oxidation of copper, indicating that the overpotential is controlled by the step corresponding to the formation of $Cu(I)CO_2^-$ intermediate.

Introduction

The rising emissions of CO_2 are one of the major threats our society is currently facing. To mitigate these emissions, the anthropogenic cycle must be closed. One of the most attractive solutions would be to use CO_2 as feedstock to make usable fuels or valuable carbon chemicals.[1] Numerous ways can be envisioned to do so, but among them the electrochemical reduction emerges as one of the most appealing due to its operating conditions (room temperature, ambient pressure, neutral pH) that makes it sustainable if coupled with a renewable source of energy.[2] Unfortunately, in aqueous media, the CO_2 reduction reactions forming CO, formic acid or other fuels often compete with the two electron reduction reaction forming H_2 from H^+, namely the hydrogen evolution reaction (HER). This competition between the CO_2 reduction reactions (CO_2RR) and HER is explained by the first electron transfer step to form the $CO_2^{\bullet-}$ radical from CO_2 ($CO_2 + e^- \rightarrow CO_2^{\bullet-}$) that requires very low potential and which greatly limits the CO_2RR in favor to the HER on the surface of many electrocatalysts.[3] Hence, even though the standard potential to form valuable fuels such as CH_4 (8 electron reduction) or C_2H_4 (12 electron reduction) in water through CO_2RR is slightly positive ($E°CO_2/CH_4$ = 0.17 V vs. RHE and $E°CO_2/C_2H_4$ = 0.08 V vs. RHE), the overpotentials associated with these reactions are often found to be very large and close to 1 V. The design of cost-effective and efficient CO_2RR catalysts is therefore of prime importance. Following the pioneering work by Hori et al in 1985,[4–6] many researches have been focusing on metals as CO_2RR catalysts and especially on copper surfaces since CH_4 and C_2H_4 have been demonstrated to be the major products formed at potentials below -0.9 V vs. RHE (-1.3 V vs. NHE at pH 6.8).[7–9] In addition to CH_4 and C_2H_4, CO and formic acid were found as CO_2RR products at potentials comprised in the range of -0.9 to -0.7 V vs. RHE, while at potentials above - 0.7 V vs. RHE the HER becomes the major reaction. Other metals such

as Au, Zn, Ag, Ni or Pd were also studied and CO_2RR products such as methanol, CO or formic acid were often found to be formed at low potentials below -1 V vs. RHE.[6,10–14]

Hence, even though our understanding of the CO_2RR mechanism on the surface of copper catalysts has made great progresses since the early works,[15–19] only few compounds were found to have a CO_2RR activity, calling for a better control of copper surfaces and morphologies so as to enhance its activity and selectivity. Following a classical electrocatalysis approach, Cu nanoparticles (NPs) were tested as CO_2RR catalysts in order to increase the active surface.[20,21] Unfortunately, the size decrease is accompanied with the increase of under-coordinated sites on the surface of Cu NPs which are very active for HER and also favor the formation of CO as CO_2RR products over CH_4 of C_2H_4. New approaches have thus been developed very recently to tackle this limitation,[22–24] and among them the formation of an oxide layer on the surface of Cu or other metallic catalysts has been proven to lead to an enhanced CO_2RR activity at relatively low overpotentials.[25–29] Nevertheless, the major CO_2RR products when using such oxidized surface are CO and formic acid which are formed at potentials in the range of -0.3 to -0.7 V vs. RHE[25] and almost no CH_4 and C_2H_4 are detected at potentials for which they are formed on the surface of bare Cu (≈ -1 V vs. RHE). These results were further reproduced on Cu_2O films for which the orientation was found to have no influence on the selectivity which is instead dependent on the thickness of the Cu_2O layer.[30] This observation strongly suggests a sacrificial reduction of the Cu_2O layer during the CO_2RR process following Scheme 1, but to date the exact mechanism remains elusive. Hence, the electrochemical formation of fresh Cu surfaces with controlled morphologies and surface roughness as well as particles size and density appears to be a key factor influencing the CO_2RR activity which also presumably controls the local pH which is of prime importance for the hydrocarbons selectivity.

Scheme 1

$$Cu(I) + e^- \overset{E^\circ}{\rightleftharpoons} Cu(0) \quad (1)$$

$$Cu(0) + CO_2 \overset{K_1}{\rightleftharpoons} Cu(I)CO_2^{\bullet -} \quad (2)$$

However, inspired by the homogeneous molecular catalysis in aprotic media for which the metallic center of the catalyst acts as a redox and adsorption center,[31,32] as well as intrigued by the redox behavior of heterogeneous catalysts such as Pd surfaces which is modified in the presence of CO_2,[10] we decided to investigate the synergetic effect of CO_2 adsorption and reduction on the redox behavior of copper, and vice and versa (Scheme 1). Unfortunately, aside from the Cu_2O reduction to Cu^0 mentioned earlier, only few examples of metallic copper formation from the reduction of a solid exist. Nevertheless, an interesting example of copper redox in solids can be found in the Li-ion batteries field for which some layered materials containing copper cations, such as $Cu_{2.33}V_4O_{11}$, were shown to extrude metallic copper upon Li insertion.[33,34] This reversible copper redox has been demonstrated in a variety of vanadates at a potential varying from 1.5 to 3 V vs. Li^+/Li (-1.5 to 0 V vs. SHE) which matches well with the standard redox potential associated with CO formation from CO_2 for instance (E^0 = -0.106 V vs. SHE) (Figure 1). However, no demonstration of copper extrusion has been made so far in aqueous environment with H^+ playing the role of Li^+ as insertion ions to trigger the Cu^0 displacement. Using the copper vanadates family, rather than focusing on the kinetics of the CO_2 reduction reaction which may be impacted by numerous factors, we aim at understanding if, similarly to homogeneous catalysis,[35] the onset potential at which CO_2RR occurs follows the standard potential $E°(Cu^+/Cu°)$ for the different catalysts.

In this work, rather than giving a full description of the mechanism at play for reducing CO_2 on the surface of copper-based electrocatalysts and analyze the products formed upon reduction which is out of the scope of this paper and summarized elesewhere,[36] we decided to focus on unraveling the effect of copper redox on the adsorption of CO_2. For that, we synthetized three copper vanadates, namely $Cu_{2.33}V_4O_{11}$, $Cu_2V_2O_7$ and $Cu_5V_2O_{10}$ and first studied their redox behavior in aprotic solvent under Argon and CO_2 atmospheres. We also investigated the CO_2 adsorption and desorption process on the surface of metallic copper formed upon extrusion and we compared them with CuO and Cu_2O. We also observe the synergy existing between the CO_2 adsorption/desorption process and the reversibility of the copper redox. Finally, we studied the redox behavior of these vanadates in aqueous media under Argon and CO_2 as well.

Experimental

Single phase $Cu_{2.33}V_4O_{11}$ was prepared by reacting stoichiometric amounts of Cu_2O, V_2O_4 and V_2O_5 under vacuum at 540°C. $Cu_2V_2O_7$ and $Cu_5V_2O_{10}$ were prepared by reacting stoichiometric amounts of CuO and V_2O_5 at 620°C and 700°C, respectively, under air. Commercial CuO and Cu_2O (Alfa-Aesar, 99%) were used as received.

Electrochemical studies in organic solvent were carried out in Swagelok-type cells with Li metal counter electrode and LP30 electrolyte (BASF) which were assembled in an argon filled glove box. The active material was ball milled with 20 %wt carbon black (Super P, Timcal) using SPEX ball mill for 20 minutes. After assembly and before the electrochemical measurements, the cells initially containing argon are filled with pure CO_2 after a pumping-

filling procedure repeated at least three times and equilibrated for 8 hours prior to electrochemical measurements.[37,38]

Electrochemical measurements in aqueous solution were carried out by drop casting an ink made by mixing THF (Sigma-Aldrich 99.9%) with the vanadate powder and ethylene black carbon (Alfa Aesar 99.9%) in a 5:1 weight ratio as well as Nafion binder (5% weight, Ion power). For the galvanostatic discharge, 200 μg of powder is drop-casted onto the surface of carbon paper previously washed with ethanol. For the cyclic voltammetry study, glassy carbon electrodes with a diameter of 0.196cm² were used as support with a loading of active material of 50 μg per electrode. Measurements were performed in glass cell previously cleaned by acid treatment followed by boiling in water for 2 hours. PINE Instrument rotating device was used at 1600rpm. A solution of 0.1 M $KHCO_3$ was used and saturated with argon for 1 hour. For measurements in CO_2 containing atmosphere, CO_2 was bubbled in the same electrolyte for 1 hour until the pH reaches 6.8. No special care was paid to pre-electrolysis of the electrolyte.

Results and discussion

Batteries were assembled in argon atmosphere before to be filled with CO_2. The pressure was monitored, using a setup described elsewhere,[37,38] during the discharge (Li insertion and Cu^0 extrusion) and the charge (copper cations re-insertion) and the corresponding curves are plotted in Fig. 2 (curves under Argon can be found in Fig. 1). For $Cu_{2.33}V_4O_{11}$ (Fig. 2a), a pressure drop is monitored during the reduction process, indicating the specific adsorption of CO_2 starting at 2.6 V vs. Li^+/Li, potential at which Cu^0 particles are freshly formed. The

pressure then stabilizes at the end of the discharge. When compared to the cyclic voltammetry recorded under argon, the reduction peaks are not modified by the presence of CO_2, indicating that the vanadate host structure doesn't interact with CO_2. The same measurements made with $Cu_2V_2O_7$ and $Cu_5V_2O_{10}$ show a similar pressure drop concomitant with the second redox peak which corresponds to the formation of metallic copper particles and specific adsorption of CO_2 (Fig. 2b and 2c). Hence, these measurements demonstrate the redox at which metallic copper particles are formed control the CO_2 adsorption onto the copper catalyst.

Nevertheless, the subsequent oxidation process largely differs for $Cu_{2.33}V_4O_{11}$ under CO_2 when compared to the redox measured under argon. Indeed, a first oxidation peak at 2.75 V without concomitant pressure evolution is first observed. Then, a second oxidation peak at 3.1 V comes along with a pressure increase, indicative of gas release. We could exclude the effect of carbon additives and/or other cell components on the CO_2 consumption or electrolyte decomposition by demonstrating that no pressure evolution was recorded for classical Li insertion materials such as $LiFePO_4$ measured under similar conditions or for $Cu_{2.33}V_4O_{11}$ cycled under Argon. Hence, the gas pressure increase observed for $Cu_{2.33}V_4O_{11}$ during the Cu^0 oxidation and the insertion of copper cations back into the vanadate host structure upon charge during the second oxidation event is related to the desorption of species formed after the CO_2 specific adsorption onto metallic copper particles while the first oxidation peak could be related to oxidation of species formed upon discharge and is associated with no gas release. Hence, not only the CO_2 adsorption is concomitant to the reduction of copper into Cu(0) but also modifies the potential at which Cu(0) is reoxidized and during which gas is released. Therefore, these results suggest that copper oxidation state and/or environment are modified by the adsorption of CO_2, resulting from the initial

formation of a species which would be qualified in homogeneous catalysis as $Cu(I)CO_2^{\bullet-}$ adduct. Interestingly, it was previously shown that the initial adduct $Cu(I)CO_2^{\bullet-}$ can be further reduced in the presence of H^+ to form CO and H_2O when using either proton-containing electrolytes, either aqueous as employed for CO_2 reduction on the surface of metallic copper[5,39] or aprotic in the presence of an acid as often used for homogeneous CO_2 reduction[3]. Nevertheless, in the absence of proton source, the Lewis acid Li^+ could play this role, as studied for iron-porphorine homogeneous catalysts in aprotic solvent[40], and eventually form Li_2O and CO upon reduction. However, the amorphous nature of Li_2O formed upon reduction for conversion transition metal oxide materials usually prevents its detection by XRD,[41] and XPS analysis carried out in this work failed at uniquely detect its presence. Another possible pathway would be the re-oxidation of the surface of metallic copper into CuO_x triggered by the absorption of CO_2 and the formation of gaseous CO through an internal redox. Observing that the oxidation peak of Cu^0 is significantly decreased in CO_2 atmosphere and also shifted in potential (Fig. 2a) and that the molar CO_2/Cu^0 ratio is very high for a surface effect, this mechanism could be plausible. However, the desorption occurring at high potential upon oxidation would in contrary indicate that the $Cu(I)CO_2^{\bullet-}$ adduct is not reduced further upon reduction to form either Li_2O or CuO_x and that the CO_2 release is triggered by its oxidation. Hence, more has to be done to uniquely assign the overall reduction mechanism which for now remains in part elusive. Nevertheless, this study suggests that the specific adsorption of CO_2 onto freshly electrochemically formed metallic copper surfaces upon reduction follows the formation of a species which could be described as $Cu(I)CO_2^{\bullet-}$. Bearing in mind that the first electron transfer to CO_2 is considered as potential limiting step, modulating the redox potential of $Cu^+/Cu°$ redox couple which controls the formation of $Cu(I)CO_2^{\bullet-}$ appears as a viable strategy to reduce the overpotential

related to the specific adsorption of CO_2 onto metallic copper surface. Finally, no pressure increase is observed upon oxidation for Cu_2V_2O7 and $Cu_5V_2O_{10}$, in contrast to $Cu_{2.33}V_4O_{11}$. As discussed in previous work, this can be explained by the fact that the host vanadate structure doesn't retain its crystallinity upon copper extrusion which modifies the copper cations reversible re-insertion into these two vanadates upon oxidation,[34] further demonstrating that the copper redox is necessary for the gas desorption process.

Comparing the electrochemical results obtained for the three copper vanadate compounds with the results obtained for CuO, a similar pressure drop during the formation of Cu^0 corresponding to the specific adsorption of CO_2 is recorded (Fig. 3a). Looking into details in the CO_2 adsorption on the CuO electrode, it clearly appears that the strongest adsorption, i.e. the strongest pressure drop, is concomitant with the reduction of Cu^+ into Cu^0 at 0.8 V vs. Li^+/Li and not with the reduction of Cu^{2+} into Cu^+ above 1 V,[41] further supporting the synergy of both metallic copper formation and CO_2 adsorption. Now looking at the Cu_2O behavior that shows only the Cu^+/Cu^0 redox (Fig. 3b), it becomes clear that the pressure drop is indeed related to the reduction of Cu^+ and the formation of metallic copper at 1.1 V vs. Li^+/Li. Moreover, as largely documented in the Li-ion battery field,[41] CuO and Cu_2O show poor reversibility for the conversion reaction which translates again in the observation that no gas evolution is seen in oxidation (Fig. 3a and 3b). This demonstrates that CO_2 is strongly bound to the electrochemically formed metallic copper surface and that only the copper oxidation can trigger the desorption process. Eventually, one can here recognize one of the major key feature of Cu surfaces, namely the strong binding energy for CO (around -0.7 eV)[8] which was demonstrated as being key for controlling the product selectivity.[42] Hence, when the potential is kept very low, the strong CO binding on the Cu^0 surface pushes towards the formation of C1 or C2 compounds[16] without premature CO desorption while when the

potential is kept close to the Cu^{+}/Cu^{0} redox potential a facile CO desorption can occur as observed for Cu_2O surfaces.[25] This explains the very high selectivity observed for Cu_2O surfaces towards the CO_2 reduction and the formation of CO or formic acid at relatively high potential (low overpotential) while metallic Cu tends to be selective for CO_2 at much lower potential.[4,7,25,30] Unfortunately, no XPS analysis could be carried out for these compounds owing for the well-known organic electrolyte decomposition and the solid electrolyte interface (SEI) formation[43] occurring at low potential for conversion compounds which often prevents to carefully study the reduction product formed in Li^{+}-containing organic electrolyte.[41,44]

As seen in Figs. 2 and 3, even though the pressure starts to drop when the metallic copper particles are formed, the pressure does not stabilize immediately, which clearly emphasizes kinetic limitations. We therefore study the kinetics of the CO_2 adsorption on the surface of freshly formed metallic copper particles by varying the scan rate during the cyclic voltammetry experiments in CO_2 atmosphere for $Cu_{2.33}V_4O_{11}$ (Fig. 4). For that purpose, the CO_2/Cu molar ratio was calculated from the pressure evolution. First, a dependence for the metallic copper formation itself with the scan rate is measured. While decreasing from 0.05 mV/s to greater scan rates results in a shift of the reduction peak to lower potentials which could be explained by the rate-dependence for the size of metallic copper particles formed upon reduction, no clear dependence could be observed at greater scan rate (between 0.1 and 0.2 mV/s). Moreover, the peak intensity doesn't follow a linear trend with the scan rate, indicating that the process is presumably not diffusion limited. Nevertheless, the oxidation process is very sensitive to the scan rate, and in particular the intensity ratio between the first oxidation peak at around 2.8 V vs. Li^{+}/Li, previously ascribed to the metallic copper oxidation and its re-insertion into the vanadate framework, and the second oxidation peak

that corresponds to a gas desorption process at around 3.1 V vs. Li^+/Li. In details, the second peak grows with decreasing scan rate. We then quantified the amount of CO_2 consumed during the reduction by looking at the evolution of the gas pressure and normalized it by the amount of copper atoms as given by the electrode loading.[38] Hence, the pressure drop monitored during the reduction process and assigned to CO_2 adsorption on the surface of metallic copper particles largely increases with the scan rate from 0.08 mol CO_2 / mol of Cu at 0.2 mV/s to 0.28 mol CO_2 / mol of Cu at 0.05 mV/s. This indicates that the kinetics associated with the CO_2 adsorption is indeed very slow and must certainly be limiting. Moreover, this increase of CO_2 adsorption is directly correlated with an increase of the gas desorption, i.e. a pressure increase during the oxidation process from 0.01 mol gas desorb / mol of Cu at 0.2 mV/s to 0.21 mol gas desorb / mol Cu at 0.05 mV/s. This further exemplifies that another key challenge facing the CO_2RR is related to the strong binding of CO on the surface of Cu and the relatively slow desorption process.

In order to further understand the potential use of the copper extrusion process as a way to selectively adsorb CO_2, we then studied the redox behavior of the vanadate phases in aqueous electrolyte. When measured in aqueous solution at pH 8.8 (Argon saturated 0.1 M $KHCO_3$) (Fig. 5a), similar trend as the one observed in organic electrolyte (Fig. 1) can be observed with the reduction potential measured for $Cu_{2.33}V_4O_{11}$ being close to 0.2 V vs RHE (-0.21 V vs. SHE and 2.83 V vs. Li^+/Li) and the one for $Cu_2V_2O_7$ close to -0.45 V vs. RHE (-0.86 V vs. SHE and 2.2 V vs. Li^+/Li). For $Cu_5V_2O_{10}$, no clear reduction peak is visible before to reach the water reduction potential. However, following the large oxidation peak observed in the anodic scan, reduction of the phase must occur at a potential overlapping with the hydrogen evolution reaction. The overall trend is that by increasing the ratio Cu/V from $Cu_{2.33}V_4O_{11}$ to $Cu_2V_2O_7$ and $Cu_5V_2O_{10}$, the reduction potential decreases in both organic solvent containing

Li^+ salt and in aqueous environment in the presence of H^+. This demonstrates that the cationic displacement and insertion phenomena previously reported with Li^+ as insertion cation can also occur with H^+. Nevertheless, when discharging (reducing) these compounds in argon-saturated aqueous solution (0.1 M $KHCO_3$ at pH = 8.8) under galvanostatic conditions, a different reduction process can be seen (Fig. 5b). For $Cu_{2.33}V_4O_{11}$ a large plateau is measured at 0.2 V vs. RHE followed by a small one at 0 V vs. RHE, corresponding to 2.7 V and 2.1 V vs. Li^+/Li, respectively, similarly to what has been reported in organic solvent with Li^+ (Fig. 1).[33] However, in contrary to what has been observed in Li^+ containing organic electrolyte for which 4 distinctive redox processes have been identified, only one plateau is observed in aqueous electrolyte and it is therefore complex to identify the successive redox reactions occurring upon reduction. Following this plateau which corresponds to 600 mAh/g, the potential drops to a potential at which hydrogen is evolved, at around -0.2 V vs. RHE. For $Cu_2V_2O_7$ and $Cu_5V_2O_{10}$, the discharge process is rather complex and a first plateau at around 0.35-0.4 V vs. RHE is observed, before the potential slowly decays but without reaching the HER potential (< 0 V vs. RHE). The capacity associated with this process (> 1000 mAh/g) is by far greater than the one observed in organic solvent at about 2.5 and 2 V for $Cu_2V_2O_7$ and $Cu_5V_2O_{10}$, respectively. As a general comment, for these three compounds, the capacity associated with the reduction process largely exceeds the capacity obtained in Li^+ containing organic solvent (270 mAh/g with 5.5 Li^+ exchanged for $Cu_{2.33}V_4O_{11}$, 350 mAh/g with 4.5 Li^+ exchanged for $Cu_2V_2O_7$ and 350 mAh/g with 7.5 Li^+ exchanged for $Cu_5V_2O_{10}$). This suggests that copper undergoes drastic dissolution and that the reduction is associated with multiple redox processes, as seen by the slight modification of the electrolyte color upon cycling.

The x-ray diffraction patterns obtained for the electrodes discharged in aqueous electrolytes are shown in Fig. 5c. For $Cu_{2.33}V_4O_{11}$, the formation of metallic Cu is clearly observed, while

for $Cu_2V_2O_7$ and $Cu_5V_2O_{10}$ the major discharge product is Cu_2O. Therefore, the reduction process previously discussed for $Cu_2V_2O_7$ and $Cu_5V_2O_{10}$ is more likely to arise from the dissolution of copper followed by the precipitation of Cu_2O rather than to a displacement reaction, since the experimental conditions (pH and potential) correspond to the domain of stability of Cu_2O in the Pourbaix diagram. Unfortunately, the large copper dissolution encountered for $Cu_2V_2O_7$ and $Cu_5V_2O_{10}$ prevents their use as model catalysts to study the effect of the formation of native Cu surface on the CO_2 adsorption and reduction mechanism in aqueous media. Even though the possibility of Cu^{2+} dissolution followed by an electrodeposition process of Cu cannot be formally excluded for $Cu_{2.33}V_4O_{11}$, the displacement reaction is confirmed when examining the discharged electrode by SEM (Fig. 5d). The large particles observed by SEM are cracked and secondary particles are found on their surfaces. Using electron dispersive x-ray (EDX) elemental mapping, the secondary particles are assigned to be metallic Cu particles, confirming the XRD result, while the remaining primary large particles do not contain copper but only vanadium. The displacement and insertion mechanism is therefore confirmed for $Cu_{2.33}V_4O_{11}$ with the general formula: $Cu_{2.33}V_4O_{11} + x\ H^+ + x\ e^- \rightarrow H_xV_4O_{11} + 2.33\ Cu$. According to the capacity obtained for the 0.2 V plateau, the amount of proton inserted (*x*) can be estimated to ≈ 11. However, this remains to be confirmed as it would correspond to a formal reduction down to Cu^0 and V^{3+}.

Finally, cyclic voltammetry were performed with $Cu_{2.33}V_4O_{11}$ - that was previously demonstrated to extrude metallic copper in aqueous solution - in argon-saturated 0.1 M $KHCO_3$ and compared with CO_2-saturated solution (Fig. 6). Interestingly, a decrease of the cathodic current is measured in CO_2 saturated solution when compared to argon saturated solution. This behavior, already reported for Pd catalysts for instance,[10,45] is associated to the

decrease of the current associated with the hydrogen evolution reaction (HER) due to the specific adsorption of CO_2 onto the electrochemically formed copper particles. The CO_2 reduction reaction being kinetically limited, it results in a limited catalytic current compared to the HER current. This further demonstrate that electrochemically formed copper surfaces are indeed electrochemically active for the CO_2 reduction reaction due to the specific adsorption of CO_2 associated with the Cu^+/Cu^0 redox. Unfortunately, since the extrusion mechanism induces large mechanical stresses as seen by SEM in Fig. 5d, no reliable electrolysis measurements were possible due to the poor mechanical stability of the $Cu_{2.33}V_4O_{11}$ electrodes upon test. However, the behavior observed in oxidation indicates that similarly to what was previously observed in organic solvent, the copper redox is modified with the disappearance of the peak corresponding to the Cu^0 oxidation and its reinsertion into the vanadate structure. Instead, a peak at 1 V vs. RHE is observed which could come, at this potential, from CO stripping or stripping of a chemisorbed CO_2 reduction product as previously observed for other CO_2 electrocatalysts.[46] This behavior is in agreement with the pressure increase, i.e. gas desorption, observed at 3 V vs Li^+/Li during the copper oxidation in organic solvent (Fig. 2a).

Conclusion

In conclusion, we used a series of copper vanadates as a model family to demonstrate that the specific CO_2 adsorption on the surface of copper oxide catalysts is governed by the Cu^+/Cu^0 redox process occurring at a potential corresponding to the standard potential for CO_2 reduction and the formation of CO or formic acid. The synergy between the CO_2 adsorption and the Cu^+/Cu^0 redox processes was evidenced by comparing $Cu_{2.33}V_4O_{11}$ from

this family that shows Cu^{+}/Cu^{0} redox couple with CuO that shows both Cu^{2+}/Cu^{+} and Cu^{+}/Cu^{0} redox processes. This result explains the very large selectivity toward CO_2 reduction found for Cu_2O surfaces at very low overpotential. Moreover, not only the CO_2 adsorption is controlled by the copper redox, but also the copper redox itself is modified by this adsorption, suggesting either the formation of CO while metallic copper is oxidized into CuO or the oxidation of the $Cu(I)CO_2^{-}$ adduct formed upon reduction. This effect is further supported by the fact that gas release only occurs at a potential corresponding to the copper reoxidation. Eventually, by studying these phases as potential CO_2 reduction catalyst in aqueous environment, we've been able to demonstrate that the copper extrusion process can be carried out using H^{+} instead of Li^{+}. However, the copper vanadates compounds show limited stability owing from either a large copper dissolution process and/or mechanical stresses that limit their long term integrity. Nevertheless, we were able to observe a similar CO_2 adsorption and a possible CO stripping mechanism that the one observed in organic solvent. More remains to do to study the interaction existing between oxidized copper species and CO_2 upon reduction, but this work demonstrates the importance of the internal redox of copper in order to selectively absorb CO_2. Unfortunately, even if the design of solids with appropriate copper redox potential provides an interesting approach to tune the CO_2RR onset potential, this strategy doesn't easily allow for tuning the kinetics related to the CO_2RR. Hence, more remains to do to understand the key features governing the CO_2RR kinetics for heterogeneous catalysts.

Acknowledgments

The authors would like to thank P. Sautet and S. Steinman as well as M. Saubanère and M.-L. Doublet for fruitful discussions. The authors would like to thank D. Foix from IPREM Pau for

the XPS analysis and D. Alves Dalla Corte for the SEM images. A.G. and J.-M.T would like to acknowledge the ANR “ECCENTRIC” for funding.

References

1 M. Fontecave, *Angew. Chem. Int. Ed. Engl.*, 2015, **54**, 6946–7.

2 K. J. P. Schouten, F. Calle-Vallejo and M. T. M. Koper, *Angew. Chem. Int. Ed. Engl.*, 2014, **53**, 10858–60.

3 C. Costentin, M. Robert and J.-M. Savéant, *Chem. Soc. Rev.*, 2013, **42**, 2423–36.

4 Y. Hori, in *Modern Aspects of Electrochemistry*, 2008, pp. 89–189.

5 Y. Hori, A. Murata and R. Takahashi, *J. Chem. Soc. Faraday Trans. 1 Phys. Chem. Condens. Phases*, 1989, **85**, 2309.

6 Y. Hori, H. Wakebe, T. Tsukamoto and O. Koga, *Electrochim. Acta*, 1994, **39**, 1833–1839.

7 K. P. Kuhl, E. R. Cave, D. N. Abram and T. F. Jaramillo, *Energy Environ. Sci.*, 2012, **5**, 7050.

8 K. P. Kuhl, T. Hatsukade, E. R. Cave, D. N. Abram, J. Kibsgaard and T. F. Jaramillo, *J. Am. Chem. Soc.*, 2014, **136**, 14107–13.

9 R. Reske, M. Duca, M. Oezaslan, K. J. P. Schouten, M. T. M. Koper and P. Strasser, *J. Phys. Chem. Lett.*, 2013, **4**, 2410–2413.

10 R. Kortlever, C. Balemans, Y. Kwon and M. T. M. Koper, *Catal. Today*, 2015, **244**, 58–62.

11 H. Mistry, R. Reske, Z. Zeng, Z.-J. Zhao, J. Greeley, P. Strasser and B. R. Cuenya, *J. Am. Chem. Soc.*, 2014, **136**, 16473–16476.

12 T. Hatsukade, K. P. Kuhl, E. R. Cave, D. N. Abram and T. F. Jaramillo, *Phys. Chem. Chem. Phys.*, 2014, **16**, 13814–9.

13 S. N. Steinmann, C. Michel, R. Schwiedernoch, J.-S. Filhol and P. Sautet, *Chemphyschem*, 2015, **16**, 2307–11.

14 S. N. Steinmann, C. Michel, R. Schwiedernoch and P. Sautet, *Phys. Chem. Chem. Phys.*, 2015, **17**, 13949–63.

15 W. J. Durand, A. a. Peterson, F. Studt, F. Abild-Pedersen and J. K. Nørskov, *Surf. Sci.*, 2011, **605**, 1354–1359.

16 K. J. P. Schouten, Y. Kwon, C. J. M. van der Ham, Z. Qin and M. T. M. Koper, *Chem. Sci.*, 2011, **2**, 1902.

17 F. Calle-Vallejo and M. T. M. Koper, *Angew. Chemie - Int. Ed.*, 2013, **52**, 7282–7285.

18 A. A. Peterson and J. K. Norskov, *J. Phys. Chem. Lett.*, 2012, **3**, 251–258.

19 A. A. Peterson, F. Abild-Pedersen, F. Studt, J. Rossmeisl and J. K. Nørskov, *Energy Environ. Sci.*, 2010, **3**, 1311.

20 R. Reske, H. Mistry, F. Behafarid, B. R. Cuenya and P. Strasser, *J. Am. Chem. Soc.*, 2014, **136**, 6978–6986.

21 W. Tang, A. A. Peterson, A. S. Varela, Z. P. Jovanov, L. Bech, W. J. Durand, S. Dahl, J. K. Nørskov and I. Chorkendorff, *Phys. Chem. Chem. Phys.*, 2012, **14**, 76–81.

22 R. Kas, R. Kortlever, H. Yılmaz, M. T. M. Koper and G. Mul, *ChemElectroChem*, 2015, **2**, 354–358.

23 R. Kas, K. K. Hummadi, R. Kortlever, P. de Wit, A. Milbrat, M. W. J. Luiten-Olieman, N. E. Benes, M. T. M. Koper and G. Mul, *Nat. Commun.*, 2016, **7**, 10748.

24 T. N. Huan, P. Simon, A. Benayad, L. Guetaz, V. Artero and M. Fontecave, *Chem. - A Eur. J.*, 2016, **22**, 14029–14035.

25 C. W. Li and M. W. Kanan, *J. Am. Chem. Soc.*, 2012, **134**, 7231–4.

26 M. Ma, K. Djanashvili and W. A. Smith, *Phys. Chem. Chem. Phys.*, 2015, **17**, 20861–7.

27 M. Ma, B. J. Trześniewski, J. Xie and W. A. Smith, *Angew. Chem. Int. Ed. Engl.*, 2016, **55**, 9748–9752.

28 A. Verdaguer-Casadevall, C. W. Li, T. P. Johansson, S. B. Scott, J. T. McKeown, M. Kumar, I. E. L. Stephens, M. W. Kanan and I. Chorkendorff, *J. Am. Chem. Soc.*, 2015, **137**, 9808–11.

29 T. N. Huan, G. Rousse, S. Zanna, I. T. Lucas, X. Xu, N. Menguy, V. Mougel and M. Fontecave, *Angew. Chem. Int. Ed. Engl.*, 2017, **56**, 4792–4796.

30 R. Kas, R. Kortlever, A. Milbrat, M. T. M. Koper, G. Mul and J. Baltrusaitis, *Phys. Chem. Chem. Phys.*, 2014, **16**, 12194–201.

31 C. Costentin, G. Passard, M. Robert and J.-M. Savéant, *Proc. Natl. Acad. Sci. U. S. A.*, 2014, **111**, 14990–4.

32 C. Costentin, S. Drouet, M. Robert and J.-M. Savéant, *Science*, 2012, **338**, 90–4.

33 M. Morcrette, P. Rozier, L. Dupont, E. Mugnier, L. Sannier, J. Galy and J.-M. Tarascon, *Nat. Mater.*, 2003, **2**, 755–61.

34 P. Rozier, M. Morcrette, O. Szajwaj, V. Bodenez, M. Dolle, C. Surcin, L. Dupont and J. M. Tarascon, *Isr. J. Chem.*, 2008, **48**, 235–249.

35 I. Azcarate, C. Costentin, C. Methivier, C. Laberty-Robert and A. Grimaud, *submitted*.

36 J. Wu, Y. Huang, W. Ye and Y. Li, *Adv. Sci.*, 2017, **1700194**, 1–29.

37 W. Yin, A. Grimaud, F. Lepoivre, C. Yang and J. M. Tarascon, *J. Phys. Chem. Lett.*, 2017, **8**, 214–222.

38 F. Lepoivre, A. Grimaud, D. Larcher and J.-M. Tarascon, *J. Electrochem. Soc.*, 2016, **163**, A923–A929.

39 Y. Chen, C. W. Li and M. W. Kanan, 2012, 0–3.

40 I. Bhugun, D. Lexa and J. Saveant, *J. Phys. Chem.*, 1996, **100**, 19981–19985.

41 A. Débart, L. Dupont, P. Poizot, J.-B. Leriche and J. M. Tarascon, *J. Electrochem. Soc.*, 2001, **148**, A1266.

42 H. A. Hansen, J. B. Varley, A. A. Peterson and J. K. Norskov, *J. Phys. Chem. Lett.*, 2013, **4**, 388–392.

43 M. Gauthier, T. J. Carney, A. Grimaud, L. Giordano, N. Pour, H.-H. Chang, D. P. Fenning, S. F. Lux, O. Paschos, C. Bauer, F. Maglia, S. Lupart, P. Lamp and Y. Shao-Horn, *J. Phys. Chem. Lett.*, 2015, **6**, 4653–72.

44 P. Poizot, S. Laruelle, S. Grugeon, L. Dupont and J. Tarascon, *Nature*, 2000, **407**, 496–499.

45 R. Kortlever, I. Peters, C. Balemans, R. Kas, Y. Kwon, G. Mul and M. T. M. Koper, *Chem. Commun.*, 2016, **52**, 10229–10232.

46 D. A. Torelli, S. A. Francis, J. C. Crompton, A. Javier, J. R. Thompson, B. S. Brunschwig, M. P. Soriaga and N. S. Lewis, *ACS Catal.*, 2016, **6**, 2100–2104.

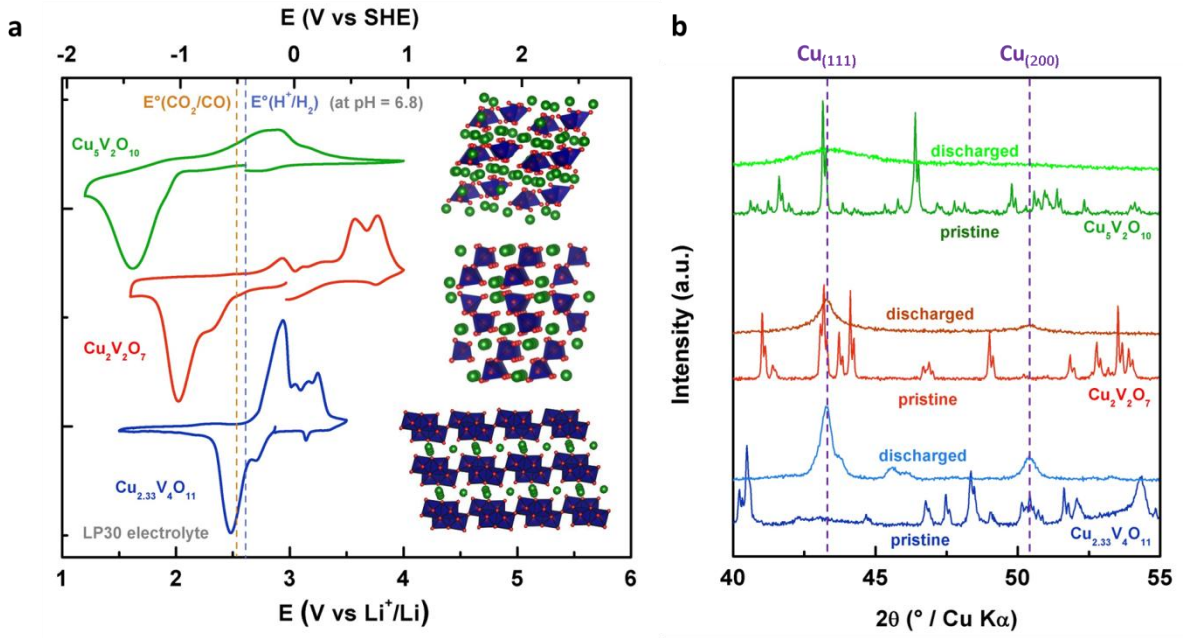

Figure 1 : **a** Cyclic voltammetry performed at 0.2 mV/s in organic electrolyte LP30 (EC :DMC 1M $LiPF_6$, LP30) for $Cu_{2.33}V_4O_{11}$ (blue), $Cu_2V_2O_7$ (red) and $Cu_5V_2O_{10}$ (green) as well as their crystallographic structures (in blue is represented the VOx polyhedral and in green the Cu atoms). Dashed lines represent the thermodynamical potentials $E°(CO_2/CO)$ and $E°(H^+/H_2)$ at pH = 6.8, which corresponds to the pH measured in 0.1 M $KHCO_3$ saturated with CO_2. Current is given in mA/g, with each division being 250 mA/g. **b** XRD patterns taken for the pristine samples (dark colors) and discharged samples (light colors) in LP30 at C/10 and showing the formation of metallic Cu^0 after reduction.

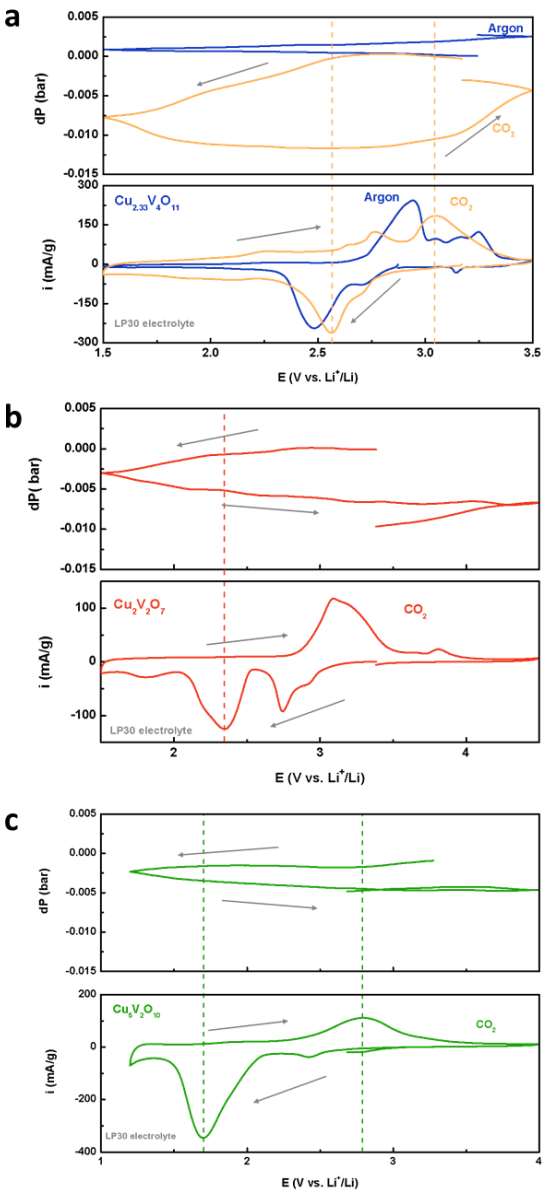

Figure 2 : Cyclic voltammetry performed at 0.05 mV/s in organic electrolyte LP30 (EC :DMC 1M $LiPF_6$, LP30) in a cell filled with CO_2 gas and where the pressure is monitored during the discharge (Cu^0 extrusion) and the charge (Cu^{2+} insertion) for a) $Cu_{2.33}V_4O_{11}$, b) $Cu_2V_2O_7$ and c) $Cu_5V_2O_{10}$.

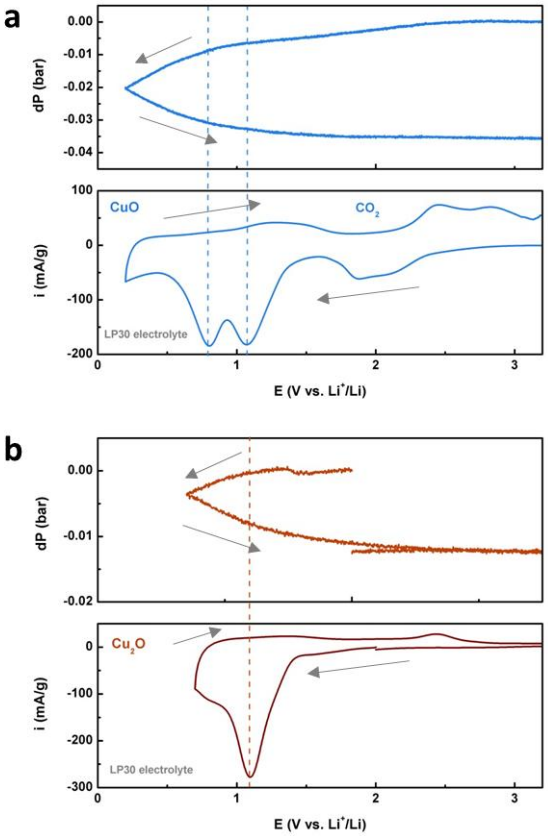

Figure 3 : Cyclic voltammetry performed at 0.05 mV/s in organic electrolyte LP30 (EC :DMC 1M $LiPF_6$, LP30) in a cell filled with CO_2 gas and where the pressure is monitored during the discharge (Cu^0 extrusion) and the charge (Cu^{2+} insertion) for a) CuO and b) Cu_2O.

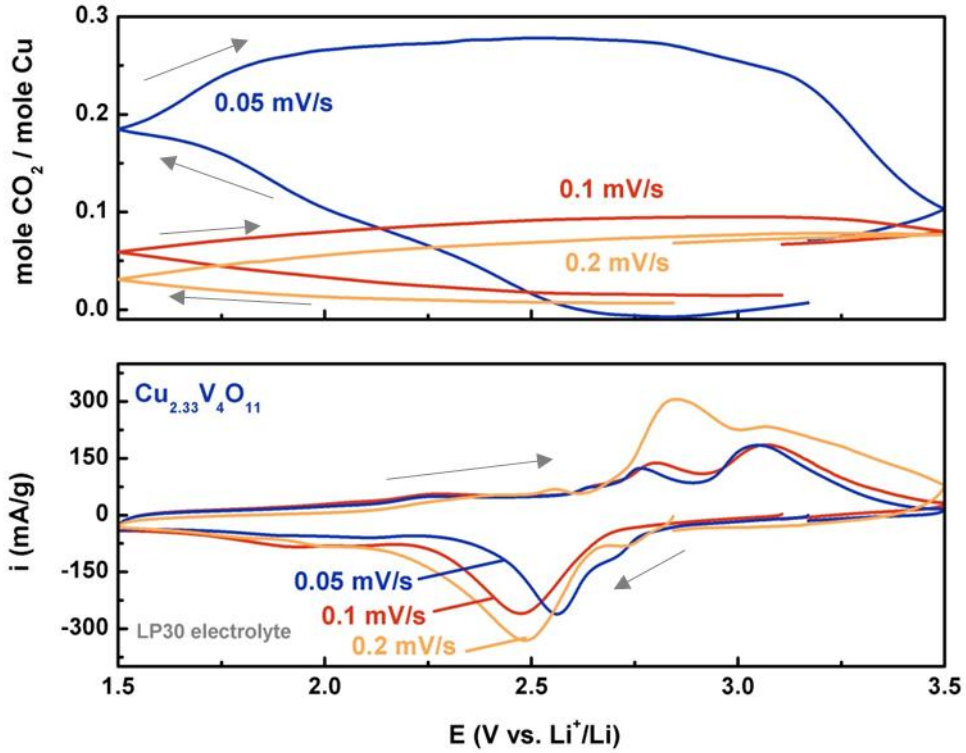

Figure 4 : **a** Cycling behavior for $Cu_{2.33}V_4O_{11}$ in organic electrolyte LP30 (EC :DMC 1M $LiPF_6$, LP30) in a cell filled with CO_2 gas and where the pressure is monitored during the discharge (Cu^0 extrusion) and the charge (Cu^{2+} insertion) at different scan rate. **b** evolution of the amount of CO_2 adsorb per mole of Cu for $Cu_{2.33}V_4O_{11}$ as a function of the scan rate as well as the difference in % (called reversibility) between the amount of adsorbed CO_2 in discharge and the amount of desorbed CO_2 in charge as a function of the scan rate.

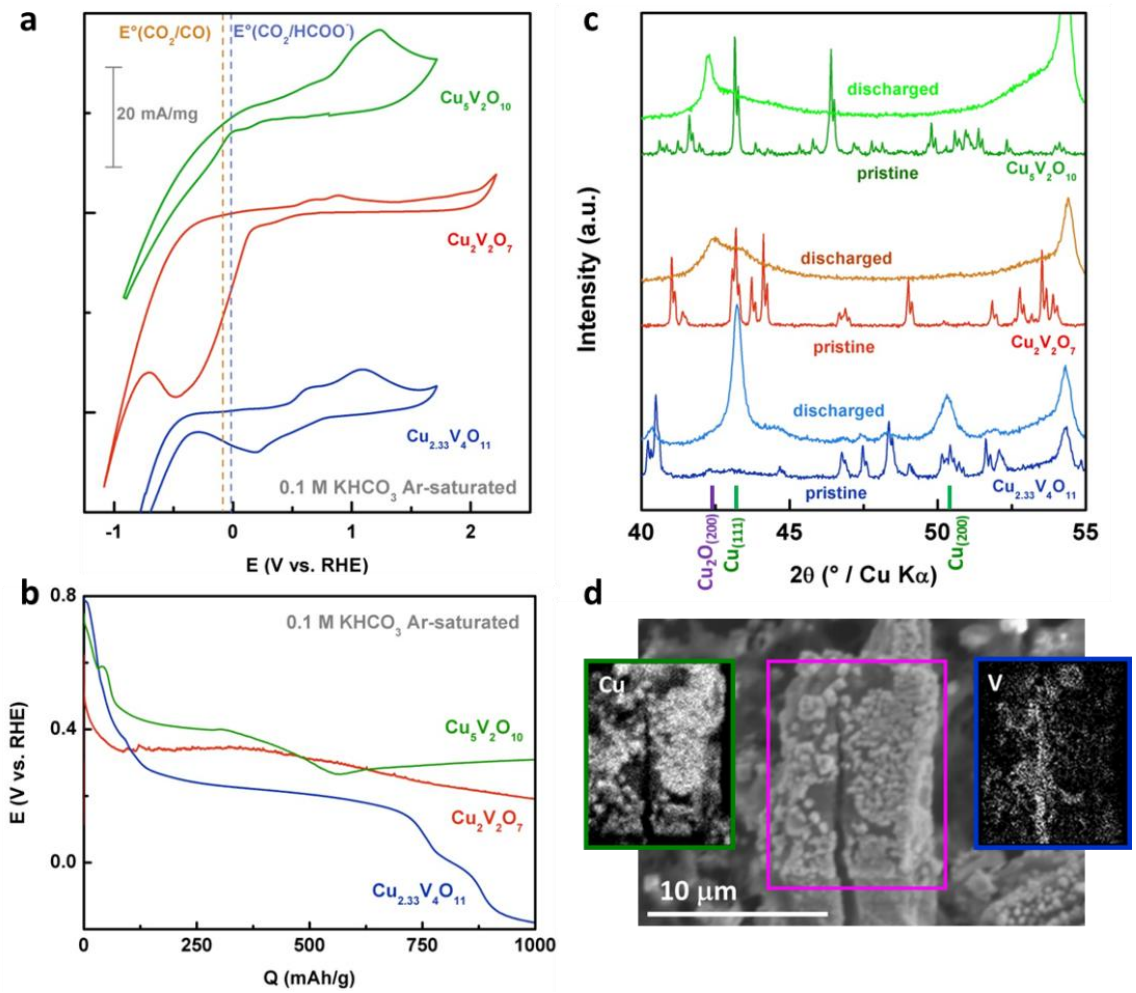

Figure 5 : **a** Cyclic voltammetry and **b** galvanostatic discharge at 1 A/g in Argon saturated 0.1 M $KHCO_3$ for $Cu_5V_2O_{10}$ (green), $Cu_2V_2O_7$ (red) and $Cu_{2.33}V_4O_{11}$ (blue). **c** XRD patterns for the pristine (dark color) and discharged (light colors) electrodes as well as Cu_2O and Cu references (peak at 54° is from the carbon support electrode). **d** SEM image for the discharge $Cu_{2.33}V_4O_{11}$ electrode as well as Cu (green, left) and vanadium (blue, right) elemental mapping on the surface of the discharge electrode corresponding to the selected area in the SEM image.

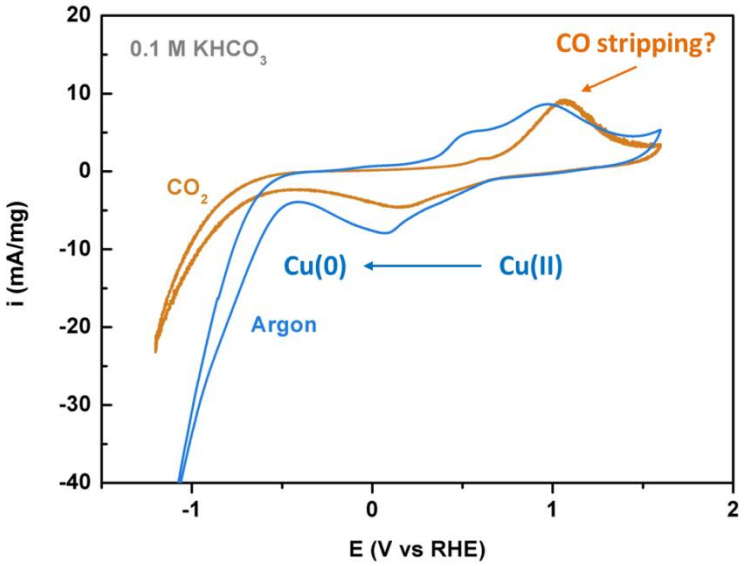

Figure 6 : Cyclic voltammetry in 0.1 M $KHCO_3$ recorded under Argon (blue) and under CO_2 (orange) for $Cu_{2.33}V_4O_{11}$ loaded onto a glassy carbon electrode.